scientific reports

Check for updates

OPEN

Autonomic correlates of osteopathic manipulative treatment on facial functional mapping: an innovative approach based on thermal imaging

Francesco Cerritelli[1,2], David Perpetuini[3], Jordan Keys[2], Arcangelo Merla[3] & Daniela Cardone[3]✉

Osteopathic manipulative treatment (OMT) has shown efficacy in various clinical conditions and age groups. Understanding its neurobiological, particularly autonomic, mechanisms of action remain limited. Preliminary studies suggested a parasympathetic effect of OMT, evidenced by heart-rate-variability analysis. A cross-over RCT on healthy adults was conducted to compare OMT with sham therapy. Thirty-seven participants underwent two sessions (OMT and sham), comprising baseline, tactile treatment, and post-touch. Novel thermal imaging data analyses in combination with seed correlation analyses (SCA) were employed to explore the OMT effects on autonomic parameters. Particularly, the sham group exhibited an elevated warming effect on the cheeks, nose, and chin. Inversely, for the OMT group a conspicuous cooling trend in the nose, but not in the cheeks and chin was observed. Considering SCA maps, the intensity of the correlation for nose tip, glabella and GSR seeds showed higher values in the OMT compared to the sham group. The comparative analysis of thermal maps and SCA results represents a significant advancement in our understanding of the physiological mechanisms underlying OMT's effects on autonomic functions. By elucidating specific patterns of temperature change, correlation intensity and specific clusters, this research provides valuable insights for optimizing clinical practice and refining theoretical models of manual therapy.

Osteopathy, a touch-based manual medicine, is widely utilized across various age groups and clinical conditions[1–6]. Numerous studies have reported positive clinical effects compared to sham treatments, placebos, standard care, or physical interventions[7–10]. Nevertheless, despite these documented clinical benefits, the precise underlying mechanisms of action for osteopathic manipulative treatment (OMT) remain an intriguing area requiring further exploration. Understanding these mechanisms is essential for advancing OMT's clinical and research applications. It remains challenging to pinpoint the primary neurobiological elements engaged during and after an osteopathic session. Existing evidence suggests that potential OMT mechanisms may be influenced by the functioning of the autonomic nervous system (ANS)[11–14], potentially involving interoceptive mechanisms[15–17]. These mechanisms could lead to a reduction in the release of pro-inflammatory cytokines[18–20], a phenomenon observed both in vitro[21] and in vivo[19], suggesting an anti-inflammatory role for OMT[12,22]. McGlone et al.[22] proposed that OMT may reduce cytokine production and sympathetic activity, triggering physiological and neurobiological events that could modulate inflammation and ANS reactivity.

The effects of OMT may be significantly influenced by the activity of the parasympathetic and sympathetic nervous systems. Ruffini et al.[11] showed that a single OMT session in healthy people produces rapid parasympathetic effects, indicating a trophotropic impact, as opposed to sham therapy and no intervention. Autonomic responses were evaluated by the authors utilizing heart rate variability (HRV)-derived measures while the subjects were in a controlled setting. In a more recent investigation, Fornari et al. found that OMT generated a chronotropic effect (lowering heart rate) and induced a sympathovagal balance[23] as compared to sham therapy in healthy volunteers exposed to laboratory-induced stress. This demonstrates the ANS's important function in the field of osteopathy. It should be mentioned, nonetheless, that the majority of research investigations looking into the

[1]Clinical Human-Based Department, Foundation COME Collaboration, 65121 Pescara, Italy. [2]NYIT College of Osteopathic Medicine, Old Westbury, NY 11568, USA. [3]Department of Engineering and Geology, University G. d'Annunzio of Chieti-Pescara, 65127 Pescara, Italy. ✉email: daniela.cardone@unich.it

function of the ANS in osteopathy have mostly concentrated on HRV, showing reduced low-frequency (LF) values, increased high-frequency (HF) values, and a lower LF/HF ratio. Considering the variety of physiological pathways that the ANS controls, this might be a restricted measure. To better understand these systems, it is crucial to combine several autonomic metrics. In order to meet this demand, this study measures regional facial temperature using thermal infrared imaging (IRI).

IRI makes it possible to accurately estimate cutaneous temperature, a stand-in for autonomic activity, using a non-contact method. Numerous research have shown that certain facial temperature patterns brought on by certain physical or psychological situations might reflect autonomic processes, proving the validity of IRI[24]. The sympathetic nervous system's activation or deactivation has been linked to temperature patterns in specific facial regions. For example, a rise in the temperature of the periorbital region signifies a fight-or-flight reaction, whereas changes in the temperature of the nose skin reflect particular autonomic consequences[25]. In particular, a drop in nasal temperature suggests a sympathetic impact, whereas an increase from baseline shows parasympathetic activation 35. Simultaneous electrodermal activity (EDA) recordings, specifically galvanic skin response (GSR) measures, have validated the validity of IRI as a method for identifying participants' psychophysiological states. The number of active sweat glands, which may be identified by facial thermal infrared imaging by the appearance of cold spots on the face, correlates with GSR signals. Multiresolution examination of the temperature signals shows phasic (event-related) and tonic (baseline and/or general) components that are closely associated with GSR sympathetic elements[26]. Consequently, tracking variations in local temperatures over time has been thought to be an appropriate approach for researching the ANS.

Recently, various regions of interest (ROIs) on the face, such as the nose tip and glabella, have been identified as significant for characterizing psychophysiological responses. However, there has been a notable gap in research regarding the functional relationships among these ROIs and the physiological basis of the connection between thermal IRI and vital signals, specifically electrodermal activity, represented by the GSR. A recent study introduces a novel methodology designed to explore the functional connections between crucial seed ROIs in thermal IRI and all pixels across the face[27]. The same approach was extended to investigate the GSR signal and its phasic and tonic components as seed signals. Through seed correlation analysis involving 63 healthy volunteers, the study identified a common pathway that regulates facial thermal functionality and electrodermal activity (the so-called butterfly pattern). Furthermore, the method was applied to a pathological case study, revealing a distinct pattern compared to the healthy cases.

Overall, this innovative methodology holds promise as a valuable tool in neurology, physiology, and applied neurosciences. It not only enhances the understanding of the relationships between facial thermal patterns and physiological responses but also has the potential to provide valuable insights into various clinical and psychophysiological contexts.

In the context of osteopathy, only two studies have employed thermal imaging. Polidori et al.[28] conducted a proof-of-concept study using a case report to explore using IRI as an additional diagnostic tool in osteopathic procedures. Their findings indicated that IRI thermography could detect immediate changes in low back pain following OMT. However, it is important to acknowledge the preliminary nature of this research, given its limitations as a case study.

To delve deeper into the impact of OMT on the ANS, a cross-over randomized controlled trial (RCT) was more recently conducted to assess the effects of osteopathic treatment compared to sham therapy on multiple autonomic parameters[29]. The study involved the collection of thermal images, HRV data, and skin conductance measurements from a group of healthy adults. Each participant underwent two sessions, one receiving OMT and the other receiving sham therapy, with one treatment session per week. Each session lasted 35 min and included 5 min of baseline measurement, 25 min of treatment, and 5 min of post-touch measurement. Notably, participants received no physical touch during the baseline and post-treatment periods. In total, 37 participants completed the study. Multivariate analysis revealed significant parasympathetic effects associated with the treatment group and the measurement epoch on thermographic data, particularly in the nose, left and right perioral regions, and the forehead. However, no significant effect was observed for the chin region. These findings align with a parasympathetic influence. Furthermore, the analyses demonstrated differences between the OMT and sham therapy groups regarding the nuHF and DFA-a1 parameters of HRV and skin conductance levels.

Nonetheless, this research serves as a foundation for additional trials to measure OMT's temporal effects using IRI accurately. The present study, therefore, seeks to address the gap by employing novel measures to investigate autonomic correlates of changes in healthy participants' baseline levels during and after OMT. Compared to the control condition, the hypothesis is that OMT will induce a more robust autonomic response.

Results

A total of fifty individuals were initially screened for participation in the study. Ultimately, 37 individuals met the predetermined inclusion criteria, provided written informed consent, and were randomly allocated to the respective intervention groups, as already reported in previous study[29], showing no statistically significant differences among the groups at baseline.

Furthermore, the type of touch felt showed similar values during the sessions (session 1: mean 8.15 ± 1.8; session 2: 8.36 ± 1.4; t = -0.56, df = 69.7, p-value = 0.58). No differences were also demonstrated for the actual type of touch provided across sessions (X2 = 0.01, p-value = 0.99).

Figure 1 presents a comparative analysis through histograms of all the pixels in the TOUCH and POST-TOUCH phases for the difference between OMT and sham groups. The distribution difference between the OMT and Sham groups, observed considering the differences between the TOUCH and POST-TOUCH phases, is relatively substantial. Student t-test showed a statistically significance difference during touch (t= -340.99; $p < 0.001$) and post-touch (t=-285.27; $p < 0.001$) phases.

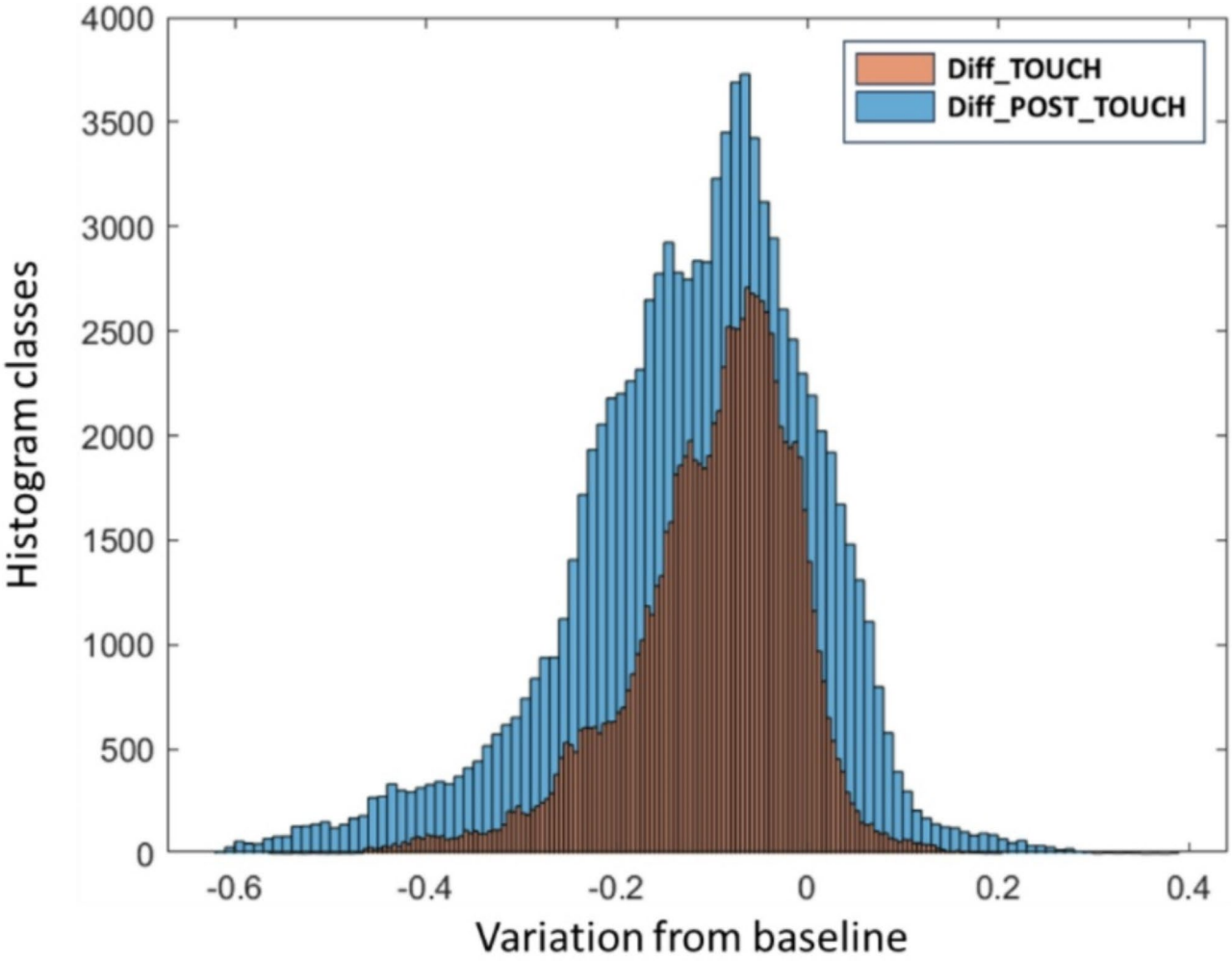

Fig. 1. Histogram distribution of the difference between the OMT and SHAM group in both TOUCH and POST-TOUCH phases.

We evaluated the difference between all the corresponding pixels of the average OMT-TOUCH image and the average SHAM-TOUCH image (Eq. 1). The same for the POST-TOUCH average images (Eq. 2).

$$Diff\_TOUCH = OMT\_TOUCH\_mean - SHAM\_TOUCH\_mean; \quad (1)$$

$$Diff\_POST\_TOUCH = OMT\_POST\_TOUCH\_mean - SHAM\_POST\_TOUCH\_mean; \quad (2)$$

Figure 2 underlines the differentiation between the OMT and sham groups, emphasizing a more substantial effect within the OMT group than the sham group. Indeed, a paired t-test showed a statistically significance difference between the TOUCH and POST-TOUCH conditions in the OMT group ($t = 151.23$; $p < 0.001$) being higher as compared to the SHAM group ($t = 75.15$; $p < 0.001$).

Figure 3 consolidates the preceding observations by showing thermal maps of the face. It notably underscores a distinct difference between the TOUCH and POST-TOUCH phases within OMT and SHAM groups. Further exploration through delta analysis unveils a characteristic butterfly pattern, corroborating prior research[27]. Specifically, the sham group exhibits an elevated warming effect on the cheeks, nose, and chin, whereas a conspicuous cooling trend is observed in the OMT group in the ROI encompassing the nose, but not in the cheeks and chin where it is possible to observe a slight increase in temperature. This temperature variance underscores the unique physiological responses triggered by the two treatment modalities.

Concerning the SCA, the resulting maps for the OMT and the sham group are reported in Figs. 4 and 5 respectively.

Comparing Figs. 4 and 5, relatively to the nosetip seed based SCA, it is possible to notice that there is a more spread correlation effect in the Sham group especially in the TOUCH condition (refer to Figs. 4a and 5a). The same effect can be retrieved also when the seed is the glabella ROI. Comparing Figs. 4c and 5c, there is a more spread effect of the correlation in the TOUCH condition. In line with these results, also the SCA relative to the GSR seed revealed the same result, with a more diffuse correlation effect in the SHAM group with respect to the OMT group.

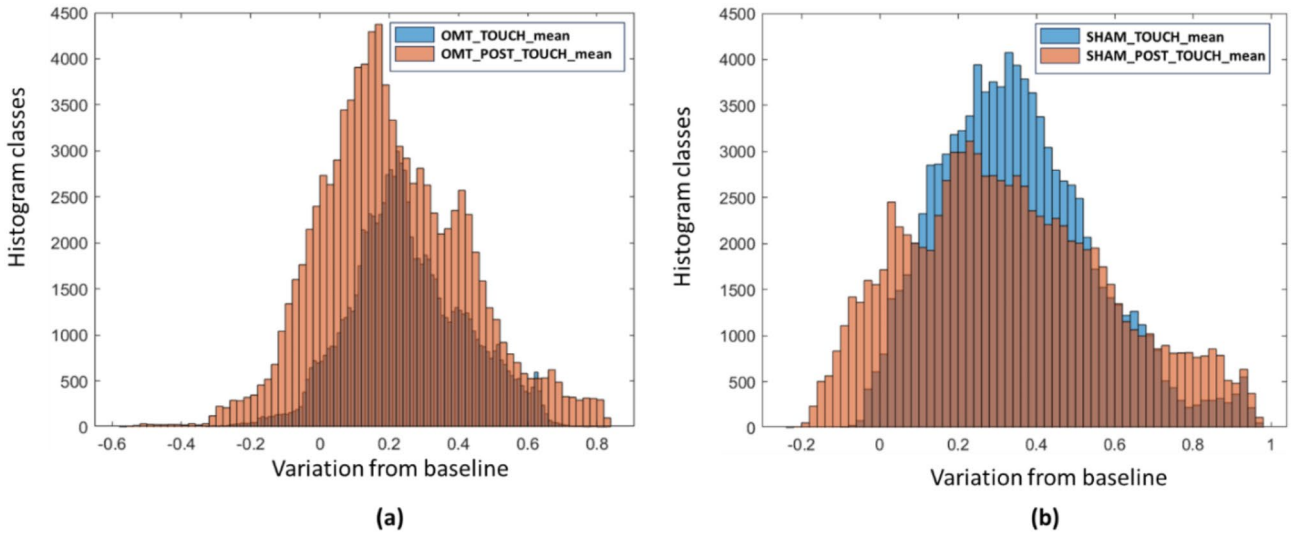

Fig. 2. Distribution of the pixel over the average images concerning: (**a**) TOUCH vs. POST-TOUCH phases in the OMT group; (**b**) TOUCH vs. POST-TOUCH phases in the sham group.

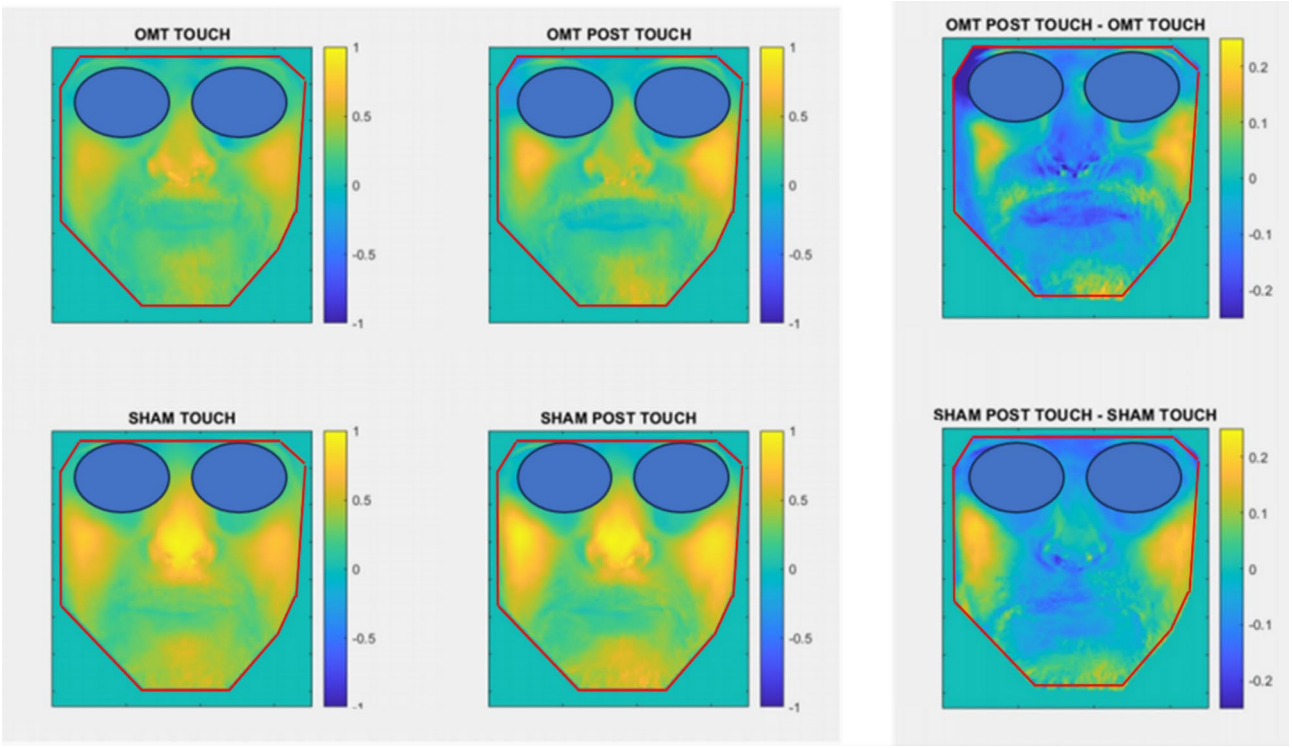

Fig. 3. Average thermal maps of the face in each one of the experimental phases (TOUCH and POST-TOUCH) and for both the experimental groups (OMT and sham). The red line represents the boundary of the warped face.

On the other hand, if we consider the intensity of the correlation in the SCA maps for nosetip, glabella and GSR seeds, we can see higher values in the OMT condition compared to the sham group.

Moreover, we performed a comprehensive statistical analysis to evaluate whether there are significant differences in correlation values within the SCA when considering salient facial ROIs.

In details a Student' t-test has been conducted over the ROIs and the specific experimental phases. Our findings reveal that the nasal region exhibits the most pronounced differentiation between the OMT and sham treatment groups (Fig. 6a). The nasal region, particularly in the touch condition, significantly influences the SCA of multiple facial areas, including the cheeks, glabella, chin, and perioral regions.

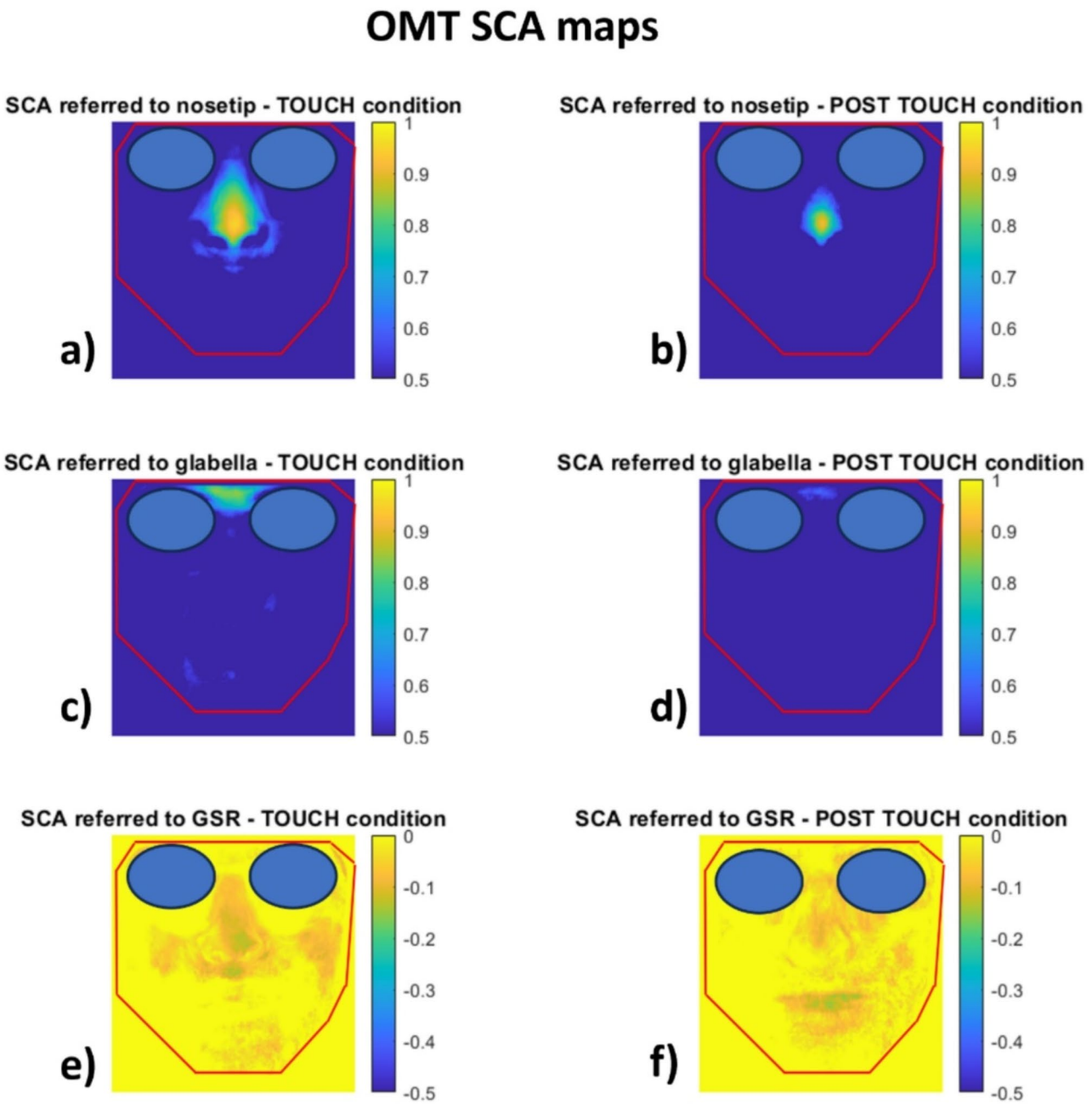

Fig. 4. SCA maps relative to the OMT group: (**a**) SCA with the nose tip seed in the TOUCH phase; (**b**) SCA with the nose tip seed in the POST-TOUCH phase; (**c**) SCA with the glabella seed in the TOUCH phase; (**d**) SCA with the glabella seed in the POST-TOUCH phase; (**e**) SCA with the GSR seed in the TOUCH phase; (**f**) SCA with the GSR seed in the POST-TOUCH phase. The red line represents the boundary of the warped face.

Moreover, the glabella region, under the influence of OMT, shows significant differentiation in the SCA values for the nose and cheeks (Fig. 6b). This indicates that the glabella's response to OMT uniquely affects the connectivity patterns of these regions, unlike the sham treatment.

These results are confirmed also by the clustering analyses. The application of k-means algorithm with $k = 5$, revealed the presence of main clusters relative to the nose and glabella areas for both OMT and sham conditions (refer to Figs. 7 and 8). Table 1 resumes also the results of the clustering procedure, revealing more concentrated clusters in the OMT condition with respect to the sham.

Discussion

The findings reported in the study provide additional insights into the effect of OMT on the function of the autonomic nervous system.

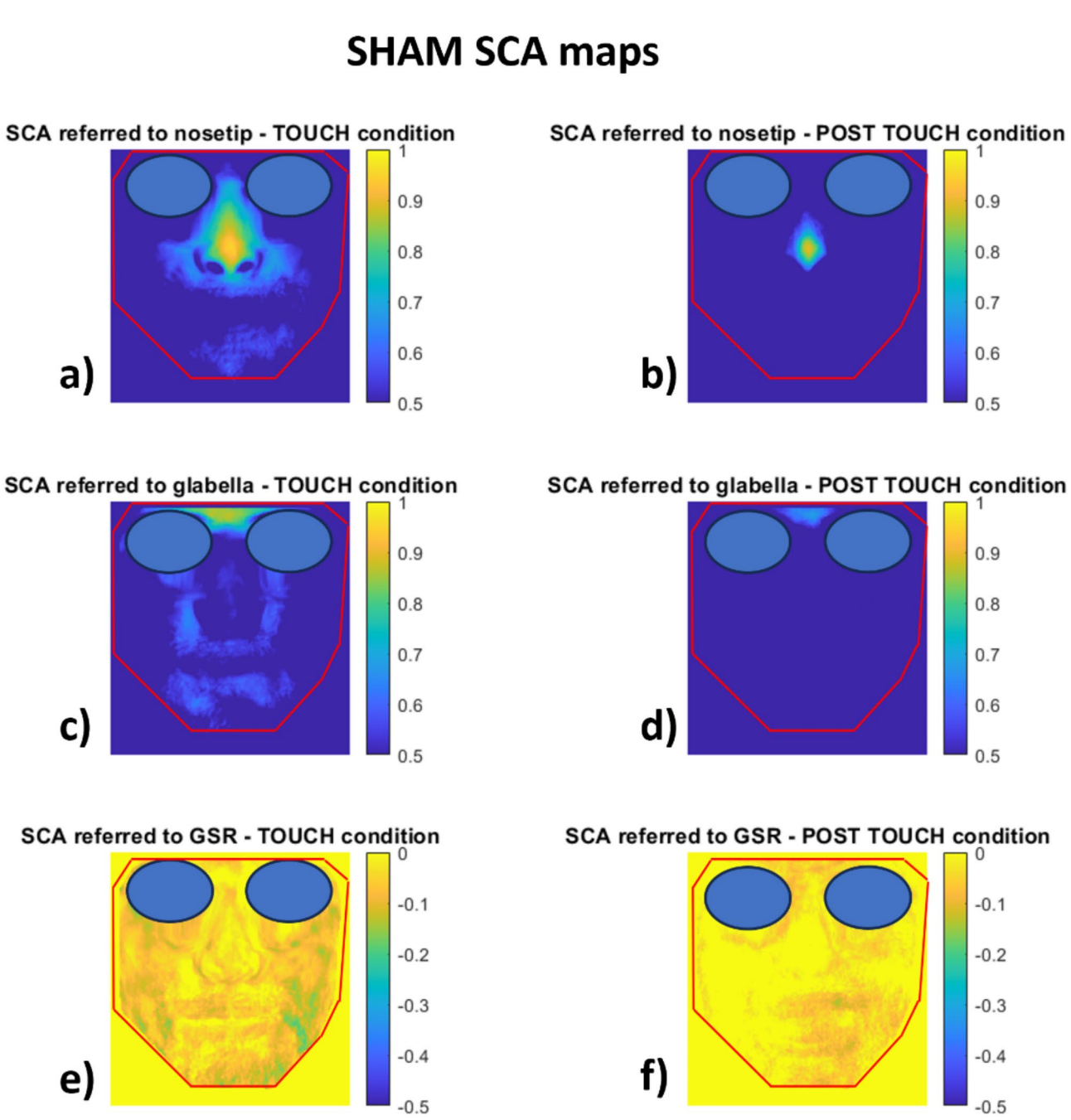

Fig. 5. SCA maps relative to the SHAM group: (**a**) SCA with the nose tip seed in the TOUCH phase; (**b**) SCA with the nose tip seed in the POST-TOUCH phase; (**c**) SCA with the glabella seed in the TOUCH phase; (**d**) SCA with the glabella seed in the POST-TOUCH phase; (**e**) SCA with the GSR seed in the TOUCH phase; (**f**) SCA with the GSR seed in the POST-TOUCH phase. The red line represents the boundary of the warped face.

The comparison of thermal maps and SCA results between groups undergoing OMT and sham treatment offers a nuanced understanding of the physiological responses elicited by OMT. This comparative analysis not only discerns specific patterns of temperature change but also unveils differences in correlation intensity across various anatomical regions. These findings are pivotal for several reasons.

Firstly, the identification of distinct patterns of temperature change provides concrete evidence of the physiological impact of OMT on the ANS. The observed variations in temperature across different anatomical regions underscore the localized effects of OMT, suggesting that specific approaches may target discrete neural pathways involved in ANS regulation. This insight challenges conventional views of OMT as a uniform intervention and emphasizes the importance of tailoring treatment approaches to individual anatomical and physiological characteristics[17].

Moreover, the differences in correlation intensity across different anatomical regions (mainly nosetip and glabella) revealed through SCA shed light on the underlying neural mechanisms through which OMT

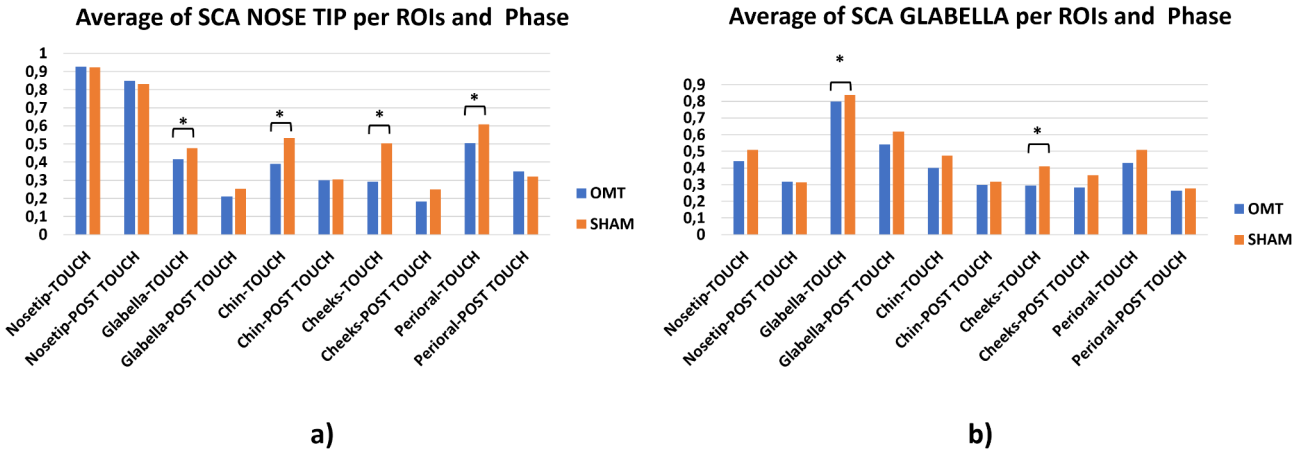

Fig. 6. Average values of the correlation values between computed over nose tip, glabella, chin, cheeks, perioral ROIs in SCA maps of the nose tip (**a**) and SCA maps of the glabella (**b**).

modulates ANS function. By pinpointing specific regions of heightened correlation activity in response to OMT, the study elucidates possible neural pathways involved in mediating autonomic responses to manual therapy. This mechanistic understanding not only enriches our theoretical framework of OMT but also provides a basis for refining treatment approaches and optimizing therapeutic outcomes.

The identification of a distinct butterfly pattern in the thermal maps, characterized by contrasting warming effects in the sham treatment group and cooling effects in the OMT group, represents a possible further advancement in our understanding of the physiological responses elicited by these treatment modalities. This observed pattern not only underscores the specificity of the physiological responses associated with each treatment modality but also provides valuable insights into the underlying mechanisms through which OMT exerts its therapeutic effects.

The presence of a warming effect in the sham treatment group suggests the activation of autonomic pathways associated with tactile stimulation or placebo effects. This finding is consistent with previous research demonstrating the capacity of sham treatments to elicit physiological responses through non-specific mechanisms[30], such as expectation[31,32], attention[33], and the release of endogenous opioids[34]. However, the distinct cooling effect observed in the OMT group suggests that OMT elicits unique autonomic responses that are not simply attributable to non-specific placebo effects.

The observed cooling effect in the OMT group may signify a modulation of autonomic activity, potentially involving either an upregulation of sympathetic activity or a downregulation of parasympathetic activity. This interpretation is consistent with the established role of OMT in modulating autonomic function and promoting physiological balance, suggesting a possible regulatory influence on vegetative functions. Interestingly, it may be argued that an increase in temperature could indicate a pro-inflammatory phenomenon, as suggested by previous research[35,36]. Several studies have demonstrated that elevated temperature is associated with increased peripheral vascular outflow, which in the context of pain, could be linked to heightened pro-inflammatory conditions[37–39].

Therefore, based on this premise, it is plausible to hypothesize that the cooling effect observed in the OMT group could represent a modulatory mechanism with potential anti-inflammatory properties. However, further research should be warranted to formally test this hypothesis, particularly in pain patients, to elucidate the specific mechanisms underlying the observed physiological responses to OMT.

The present study introduces a novel method of thermal data analysis, distinct from the traditional procedures employed by Cerritelli et al.[29]. This innovative analysis ensures a completely user-independent analysis, mitigating potential biases associated with manually selecting ROIs for analysis. By employing this new methodology, the study provides a more rigorous and standardized approach to thermal data analysis, enhancing the reliability and validity of the findings.

Furthermore, while previous studies[27] may have focused solely on the technical validation of the analysis procedure, the present study demonstrates its clinical applicability for the first time. The study extends the procedure's utility beyond technical validation to real-world clinical settings by applying the innovative analysis method to investigate the physiological responses to OMT. This advancement in methodology enhances our understanding of the physiological effects of OMT but also highlights the importance of methodological innovation in advancing research in the field.

Despite the observed cooling effect in the present study, further neurophysiological research should be warranted to elucidate the underlying autonomic mechanisms involved. It is essential to explore how OMT modulates autonomic function and influences facial temperature regulation, particularly considering the findings that contrast with previous research. By combining innovative analysis techniques with rigorous neurophysiological investigations, future studies can provide a more comprehensive understanding of the effects of OMT on autonomic regulation and thermal responses.

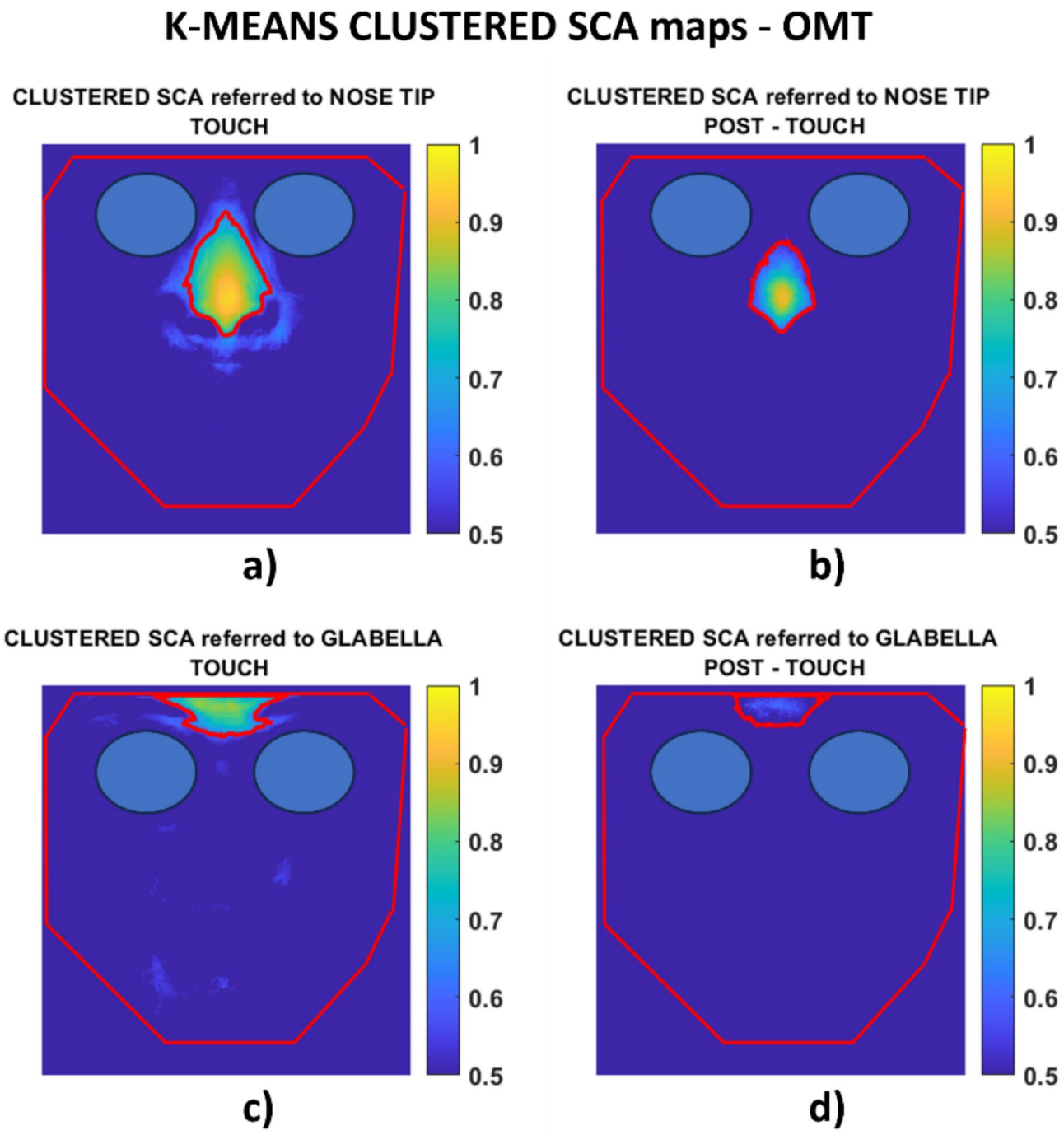

Fig. 7. k-means clustering of SCA maps for the OMT group: (**a**) clustered SCA with the nose tip seed in the TOUCH phase; (**b**) clustered SCA with the nose tip seed in the POST-TOUCH phase; (**c**) clustered SCA with the glabella seed in the TOUCH phase; (**d**) clustered SCA with the glabella seed in the POST-TOUCH phase. The red line represents the boundary of the warped face, whereas the red curved area represents the dominant cluster resulting from k-means algorithm.

Relatively, instead, to seed correlation analyses results, our study's data reveal that the nasal region exhibits unique activation patterns across all SCAs. This sensitivity is particularly pronounced during the touch condition of OMT compared to the sham treatment. These findings, consistent with existing literature on the nose's responsiveness during cognitive and emotional tasks[40,41], present an additional perspective on the role of the nasal region in neural activation.

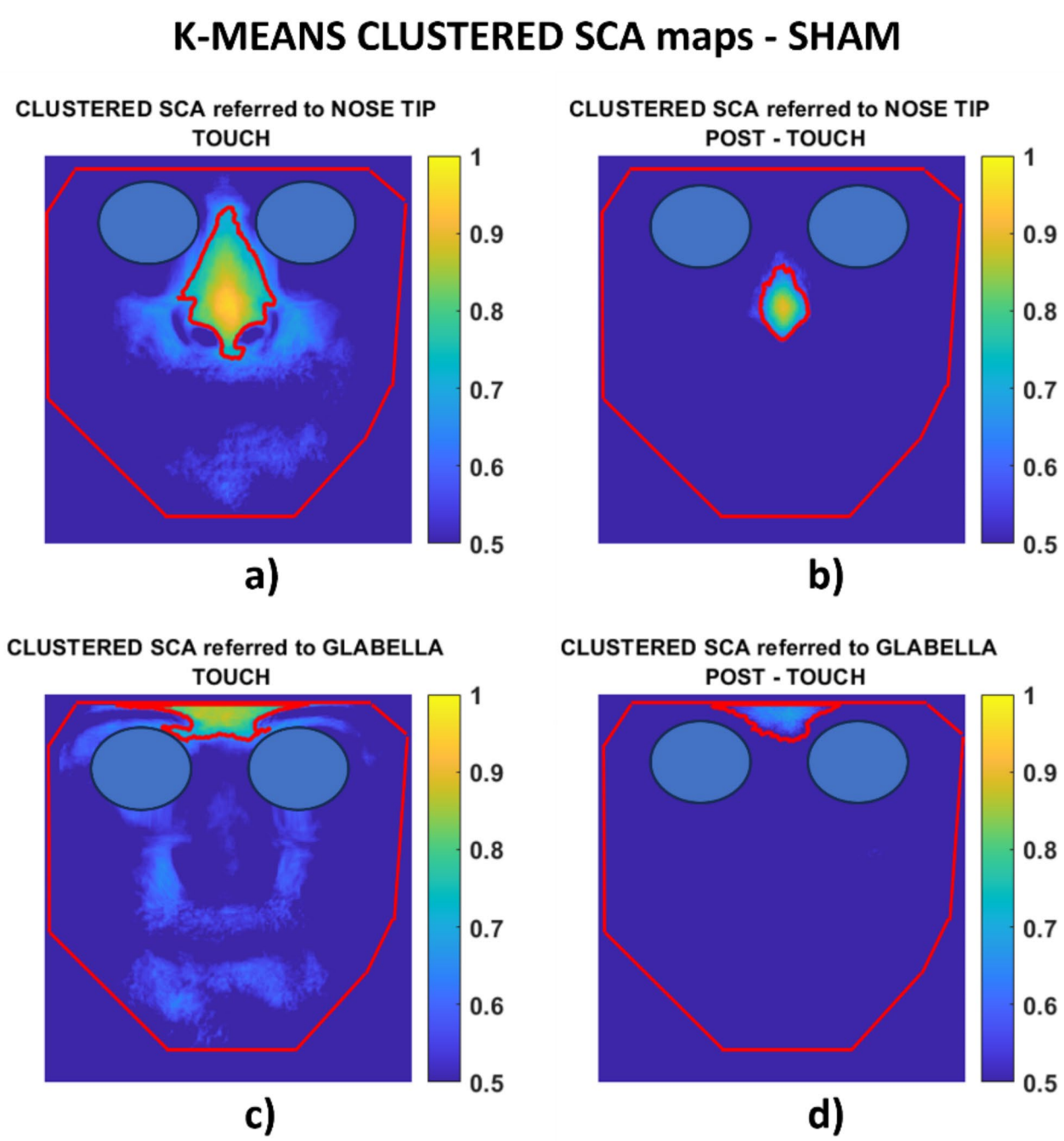

Fig. 8. k-means clustering of SCA maps for the SHAM group: (**a**) clustered SCA with the nose tip seed in the TOUCH phase; (**b**) clustered SCA with the nose tip seed in the POST-TOUCH phase; (**c**) clustered SCA with the glabella seed in the TOUCH phase; (**d**) clustered SCA with the glabella seed in the POST-TOUCH phase. The red line represents the boundary of the warped face, whereas the red curved area represents the dominant cluster resulting from k-means algorithm.

Our results not only confirm the pivotal role of the nasal region in differentiating the effects of OMT from sham treatment but also highlight the distinct impact observed in the glabella. This further supports the specificity of OMT in altering functional connectivity across various facial regions. These findings suggest a potential for OMT to modulate neural correlations nuancedly, opening new possibilities for targeted therapeutic strategies.

The glabella's significant differentiation between OMT and sham conditions, particularly in its influence on the nose and cheeks, corroborates our hypothesis regarding the activation of these regions. The activation

ROI/phase condition	OMT	SHAM
NOSE TIP / TOUCH	Centroid = 0.798 *N* = 5687	Centroid = 0.801 *N* = 6631
NOSE TIP / POST-TOUCH	Centroid = 0.680 *N* = 3487	Centroid = 0.719 *N* = 2176
GLABELLA / TOUCH	Centroid = 0.726 *N* = 2961	Centroid = 0.777 *N* = 2984
GLABELLA / POST-TOUCH	Centroid = 0.488 *N* = 2436	Centroid = 0.548 *N* = 3011

Table 1. k-means clustering (k = 5). Centroid = centroid of the main cluster. N = number of pixels in the cluster.

patterns observed in the glabella align with its known involvement in attentional tasks, which are cognitive processes that allow individuals to selectively concentrate on one aspect of the (internal) environment while ignoring other stimuli, requiring cognitive load and concentration[42].

Our findings, which align with existing literature, such as fMRI studies that demonstrate the post-treatment activation of brain areas associated with attentional control, such as right inferior frontal gyrus, which is particularly engaged in covert attention[43], provide a robust validation of our research. This alignment with established research not only strengthens our findings but also instils confidence in the potential of OMT to influence attentional tasks.

Further supporting our findings, Cerritelli et al. (2020) showed that OMT can influence activity in the right middle frontal gyrus (rMFG), enhancing precise attentional control and improving the re-orientation of attention towards endogenous stimuli22. In their study, they found that OMT led to increased activation in the rMFG, a brain region associated with attentional control, suggesting that OMT may improve internal bodily perception accuracy by facilitating the switch from external to internal focus.

In summary, the introduction of a novel analysis approach in the present study not only addresses potential biases associated with traditional methods but also demonstrates its clinical relevance for investigating the physiological effects of OMT. Moving forward, continued methodological innovation and neurophysiological research are essential for advancing our understanding of the complex mechanisms underlying the effects of OMT on autonomic function and thermal regulation.

Therefore, further research is necessary to deepen the understanding of OMT effect on temperature. Notwithstanding the fact that further and more advanced methodological analysis needs to be developed, the presence of distinct thermal patterns between the sham and OMT groups provides additional empirical evidence supporting the notion that OMT elicits unique autonomic responses compared to sham treatment. This finding has important implications for both research and clinical practice. From a research perspective, it highlights the importance of using appropriate control conditions, such as sham treatment, to distinguish specific treatment effects from non-specific placebo effects. From a clinical perspective, it underscores the potential of OMT as a targeted intervention for modulating autonomic function and promoting health. By delineating the precise physiological responses elicited by OMT, clinicians can tailor treatment strategies to target specific autonomic dysfunctions associated with various medical conditions. This personalized approach holds promise for enhancing treatment efficacy and improving patient outcomes across a wide range of disorders characterized by autonomic dysfunction, such as dysautonomia, chronic pain syndromes, cardiovascular diseases, or gastrointestinal disorders.

The study's scope was limited to investigating the immediate effects of a single osteopathic manipulative intervention on short-term measures of autonomic functions, thereby focusing solely on acute responses. Consequently, the predictive value of a single session compared to multiple sessions remains uncertain, as the sustained effects of brief treatments have not been explored. Future research should investigate the long-term stability and persistence of the observed autonomic changes. Additionally, the study recruited healthy volunteers rather than patients, potentially limiting the generalizability of the findings. It is plausible that patients with impaired autonomic tone may respond differently compared to healthy volunteers, who may exhibit no discernible effect. It would be beneficial to conduct similar studies in patients with specific autonomic disorders or other relevant medical conditions to confirm the clinical relevance of the findings. A more mechanistic understanding of the autonomic mechanisms underlying the effects of OMT is essential. Further research should aim to elucidate the specific neural pathways and physiological processes driving the observed autonomic changes. Advanced neuroimaging techniques, such as functional near-infrared spectroscopy (fNIRS) and functional magnetic resonance imaging (fMRI), could provide valuable insights when combined with continuous monitoring of autonomic parameters, including electrocardiography (ECG) and respiratory activity. Integrating these multimodal data sources would offer a more comprehensive perspective on the underlying mechanisms of OMT. Moreover, the absence of a pre-defined treatment protocol was a deliberate choice aimed at mirroring routine osteopathic clinical practice, where treatment approaches often lack rigidly pre-defined protocols. This approach allowed for an exploration of the association between technique and outcomes within real-world clinical scenarios, albeit with potential implications for standardization and reproducibility.

Methods

Experimental design and participants

The research protocol was devised for a randomized, controlled, single-blinded cross-over study, involving the recruitment of 37 healthy participants, irrespective of gender (males: 19; 40%), aged between 18 and 35

years (mean age: 27.2 ± 5.1). The demographic and clinic characteristics are reported in Table 2 showing no statistically difference at the baseline among groups. The sample size was established as follows: opting for an effect size of 0.7, coupled with an alpha value of 0.05 and a Beta of 0.80—parameters commonly employed in clinical studies—were integrated into the R statistical program to estimate the required sample size. Our aim, encompassing intraindividual and interindividual differences, led to examining a total of $n = 35$ individuals in a crossover design.

Participants had not been subjected to any pharmacological treatments in the preceding 4 weeks and had no prior exposure to osteopathic treatment. Exclusion criteria were implemented to exclude conditions that could potentially influence autonomic responses. These criteria encompassed cardiovascular, neurological, musculoskeletal, psychiatric, genetic, or congenital disorders, current pregnancy or breastfeeding, and the occurrence of menstrual flow during the session. Individuals who smoked or engaged in drug use were also excluded. Furthermore, participants were instructed to abstain from alcohol, caffeine, and cardiovascular exercise for a 24-hour period leading up to the experimental session to mitigate external confounding factors.

Participation in the study was entirely voluntary, and no financial compensation was provided to the participants.

The Institutional Ethics Committee of the University, "G. D'Annunzio" of Chieti-Pescara, granted approval for the study, and written informed consent was obtained from all participants prior to the experiment, in adherence to the principles outlined in the Declaration of Helsinki. All methods were performed in accordance with the relevant guidelines and regulations. The trial was registered on clinicaltrials.gov with the identifier: NCT03888456 (Study start date: 25/03/2019) (https://clinicaltrials.gov/ct2/show/NCT03888456).

The study was performed in the "G. D'Annunzio" of Chieti-Pescara and involved two sessions conducted over two weeks, with one session per week. Each session lasted 60 min and consisted of the following segments: a 20-minute rest period before measurements, 5 min of baseline measurement (BASELINE), 25 min of treatment (TOUCH), 5 min of post-treatment measurement (POST-TOUCH), and a final 5 min for completing post-session questionnaires. Participants did not receive any physical touch during the baseline and post-treatment periods.

Participants were randomly divided into two groups, Group A and Group B, in a 1:1 ratio for the initial session of either OMT or Sham therapy. Block randomization was employed with a block size of 9, determined by a computer-generated randomization list. Participants remained unaware of the study design, outcomes, and group allocation throughout the study.

Treatment group assignments were such that participants experienced both OMT and sham therapy sessions at different time points based on the cross-over design. In the first session, Group A received OMT while Group B received sham treatment, and in the second session, Group A received sham treatment while Group B received OMT. During the baseline, treatment, and post-treatment periods, participants were instructed to lie still with their eyes closed. Non-attendance at the second session resulted in participants being classified as drop-outs.

Both manual therapy sessions were conducted in a controlled environment with stable temperature and humidity to minimize the influence of bodily thermoregulation[24]. The sessions were scheduled at the same time of day to account for potential circadian rhythm effects. Both OMT and sham therapy sessions were administered by the same operator, a 40-year-old male with 15 years of clinical experience as a certified osteopath DO, trained according to the WHO benchmark.

A FLIR A655sc thermal camera equipped with a 640 × 480 bolometer focal plane array (FPA) and a noise equivalent temperature difference (NETD) of 50 mK at 30 °C was utilized to capture facial thermal Infrared Imaging (IRI). Simultaneously, a visible video stream was recorded using a Logitech© C920 HD PRO webcam, featuring a resolution of 1080 × 1920 pixels and a full HD lens.

Characteristics	OMT	Sham	$p > \|t\|$
Demographic			
Age	27.1 ± 5.0	27.6 ± 5.3	0.76
Female sex (%)*	13 (68)	10 (56)	0.64
BMI	22.3 ± 4.6	23.4 ± 3.3	0.40
Civil State (%)			1.00
Not-married	17 (89)	17 (94)	
Married	2 (11)	1 (6)	
Education title (%)*			0.58
High School	11 (58)	11 (61)	
Academic degree	8 (42)	7 (39)	
Clinical			
STAY-Y1	43.3 ± 4.2	45.1 ± 4.3	0.14
STAY-Y2	43.0 ± 4.5	42.5 ± 5.2	0.76

Table 2. Demographic and clinical characteristics of the OMT and Sham groups at baseline. Data are presented as mean ± standard deviation. *N (%). p-values from Student t-test. BMI, Body Mass Index. STAI, State-Trait Anxiety Inventory.

Simultaneously, the GSR was acquired from the thenar/hypothenar muscles of the non-dominant hand57 using the AD instrument Powerlab system. This system featured a low-voltage GSR amplifier, 75-Hz AC excitation, and automatic zeroing. The finger electrodes were constructed from stainless steel and secured using Velcro tape. A sampling frequency of 1 kHz was selected for data acquisition.

For each experimental session, Powerlab and thermal camera were ensured to start together the acquisition by the use of a hardware based trigger. In particular, a TTL signal was sent from the thermal camera to the Powerlab system, allowing it to start the acquisition simultaneously. Then, the GSR signal was downsampled to have the correspondence frame by frame with thermal imagery.

Osteopathic and Sham treatments

The OMT session commenced with a manual assessment to identify somatic dysfunctions based on parameters such as tissue alteration, asymmetry, range of motion, and tenderness (TART). These findings guided the subsequent osteopathic evaluation and treatment, which included techniques such as balance ligamentous techniques, balance membranous techniques, and cranio-sacral techniques[43]. Techniques involving contact with the head were excluded. The OMT session lasted approximately 25 min.

Sham therapy replicated the procedures of osteopathic care but did not involve any specific techniques. The sham session mirrored the OMT session in terms of contact time, session duration, and treatment context following the touch equality assumption paradigm[30,44,45]. It consisted of gentle static touch applied using the palms of the hands to various bodily areas, including the upper and lower limbs, pelvis, abdomen, thorax, and vertebral spine. Each area received touch for 3 to 4 min without specific attention to the region being contacted. The operator engaged in an auditory endogenous covert oriented attention task 47 and randomly determined the sequence of bodily areas to be touched.

Participants assessment

Prior to the thermography session, participants completed paper-based questionnaires. A socio-demographic questionnaire gathered baseline data on age, gender, BMI, marital status, academic degree, and type of work. Trait anxiety was assessed using the State-Trait Anxiety Inventory (STAI-Y1 and Y2)[46], and hand dominance was determined using the Edinburgh Handedness Inventory[47].

To assess the type of touch perceived by participants during the sessions, we utilized the Touch Perception Task[48]. This validated task allows for the detailed description and categorization of tactile stimuli based on participant feedback. In conjunction with the Touch Perception Task, we administered a 5-point Likert scale to classify the intensity of the touch received by participants. The scale was designed as follows: 1 = Very light; 2 = Light; 3 = Moderate; 4 = Heavy; 5 = Very heavy. Participants were asked to rate their perception of the touch immediately after each session. This dual approach allowed us to capture both qualitative and quantitative data on the tactile experiences, ensuring a comprehensive understanding of the participants' perceptions and the potential variability in tactile sensitivity across different regions of interest.

Infrared thermography data processing

To track facial landmarks on IRI, 68 specific points of interest were identified in the visible imagery using OpenFace software[49]. Subsequently, these landmarks were co-registered with the thermal IRI by estimating the geometric transformation between the visible and infrared optics, following a procedure described elsewhere[50]. Both video streams were acquired at a rate of 10 Hz to ensure temporal synchronization. The estimated facial landmark coordinates on the thermal IRI were then used to align thermal images with a reference template using a Local Weighted Mean (LWM) geometric transformation[51]. This procedure facilitated a consistent reference framework for facial regions across all subjects in terms of pixel locations, enabling precise and objective comparisons among individuals.

It is important to emphasize that the entire warping process is automated, requiring no manual intervention by a human user. This approach ensures a completely user-independent analysis, addressing potential biases associated with traditional IRI processing methods, wherein users typically manually select the ROIs for further analysis. The reliability and performance of this procedure have already been validated, with two technical publications providing in-depth assessments of its capabilities[50,51]. Specifically, the algorithm described by Cardone in 2021 demonstrated good spatial accuracy (average Root Mean Square Error, RMSE = 0.66 pixel) and temporal accuracy (RMSE = 0.81 ms) in the co-registration of visible and IR imagery[50]. This level of performance ensures reliable estimation of regional temperature (RMSE = 0.09 °C) within a defined range of head rotation (± 24.23° for yaw and ± 13.79° for pitch movements), indicating robustness to inter-subject facial geometric and anatomical variations, as well as intra-subject movement-related noise. Moreover, this technique has been successfully employed in several prior studies[52,53].

For the present study, each thermal image of every subject was aligned with the common template, commonly used in computer vision applications for face detection and recognition[50,54–57], resulting in an average of 18,000 aligned images per subject.

Galvanic skin response data processing

The GSR signal underwent filtration through a zero-lag third-order Butterworth bandpass filter (0.01–5 Hz)[58,59]. Subsequently, the signal was down-sampled to 10 Hz to align with the sampling frequency of the IRI data. This down- sampling was done to ensure data consistency between GSR and IRI.

Statistical analysis

To characterize the study population, socio-demographic data and questionnaires were examined using descriptive statistics including the arithmetic mean, standard deviation, median, percentage, and range. Student's t test and X2 were used to compared between-group data.

For thermal IRI, instead, after the alignment to the template, each of the frame of the TOUCH and POST-TOUCH sessions were normalized to the BASELINE. In detail, the mean value of the temperature of each pixel was computed over the BASELINE phase and each of the pixel of the subsequent experimental phases were subtracted to the relative BASELINE average value.

For each subject an average image for each experimental phase is then obtained. At the end, an average image among all the subjects for both OMT and SHAM conditions were obtained and for both TOUCH and POST TOUCH experimental phases. Figure 9 resumes the whole analysis pipeline.

To evaluate instead the spatial correlation of the single seed ROI (sROI) within the context of IRI and in relation to GSR signals, a specialized analytical approach known as seed correlation analysis (SCA) was developed[27,60,61].

Specifically, considering the recognized importance of certain ROIs as highlighted in the scientific literature[25,27], two distinct seed regions were selected: the nose tip (NT) and glabella (GL) (Fig. 10). For each of these ROIs, the average temperature across all pixels within the ROI was calculated, and the temporal dynamics of the signal were extracted for all video frames. This process yielded a thermal signal as depicted in Fig. 10. It is noteworthy that due to the implementation of the warping procedure on the complete dataset images, aligning them with a shared template, the positions of ROIs remained consistent across different subjects.

The same methodology was applied for the seed correlation map concerning the GSR signal. Average correlation map values were computed for all subjects, resulting in a comprehensive seed correlation map. Additionally, standard errors for the correlation maps were determined.

As reported in a previous study[29], the determination of the participant count (n) was performed before the start of the investigation. The existing literature in neuroscience, specifically in thermography, provided insights into anticipated effect size estimates, which were noted to be relatively high.

Two-tailed p-values less than 0.05 were considered indicative of statistical significance.

To investigate the impact and difference among the obtained seed correlation maps in the different ROIs of the face, the average values of the seed correlation in salient ROIs (nose tip, cheeks, glabella, chin, and perioral regions) were computed. The regions were defined as showed in the mask image reported in Fig. 11.

Lastly, a clustering analysis has been conducted on the SCA maps to objectively determine the area extent of the SCA. A k-means clustering algorithm (with k = 5) was applied to each of the average SCA maps for both the conditions (TOUCH and POST-TOUCH) and both the groups (OMT and sham). K-means clustering is an unsupervised machine learning algorithm used for partitioning a dataset into k distinct clusters based on feature

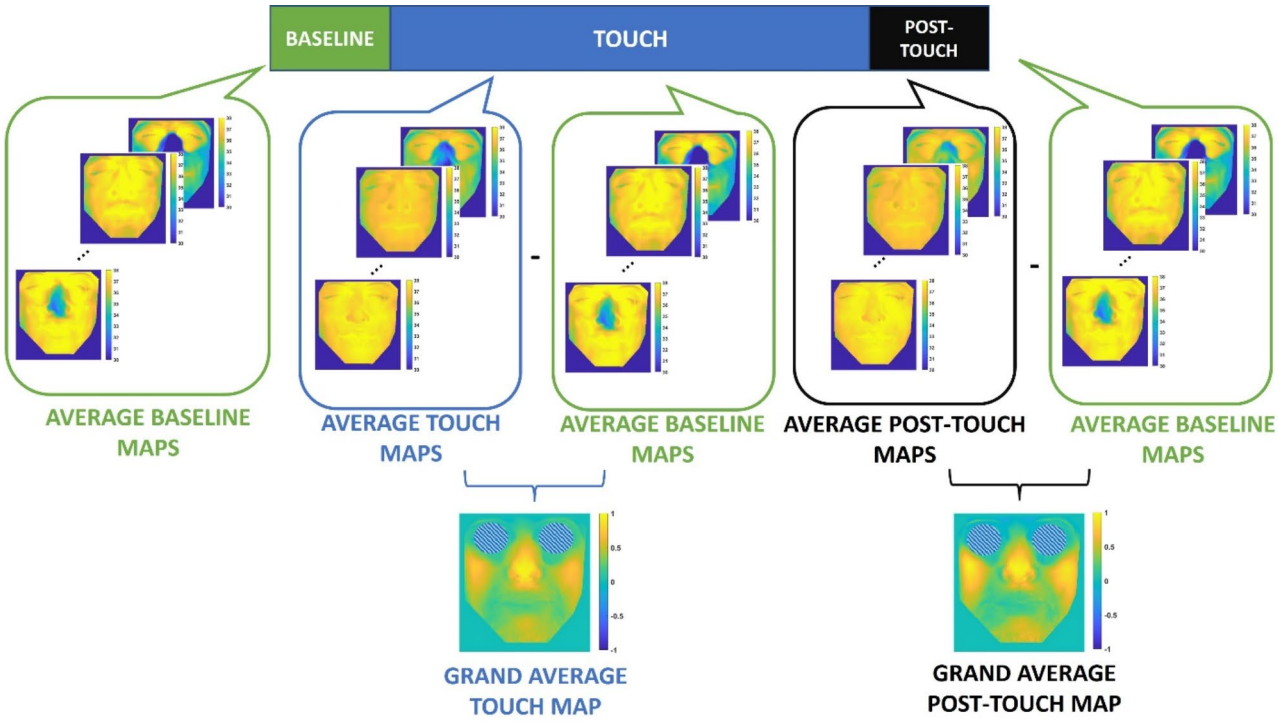

Fig. 9. Pipeline of the developed method: the warped images relative to the BASELINE phase are averaged for each subject; the average baseline image is subtracted to the TOUCH and POST-TOUCH images; the average values of the resulting images are computed for both TOUCH and POST-TOUCH phases, thus obtaining the grand-average images.

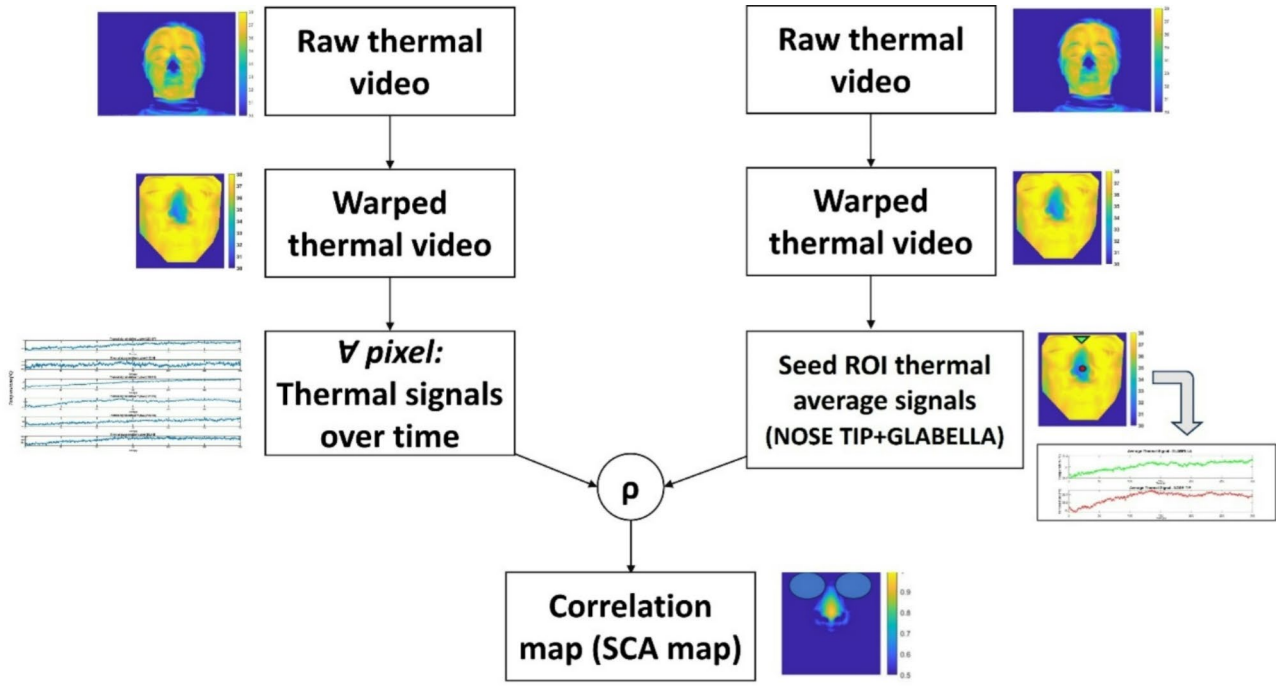

Fig. 10. Description of the method developed to obtain the SCA map.

similarity. In this study k was set to 5 and the starting centroids were equally distributed in the interval [-1,1]. After applying the k-means algorithm, the most relevant cluster was found choosing the wider area clusters. The results are reported only for the maps relative to the thermal signals since the correlations relative to the GSR signals were not uniquely clustered and were significantly lower with respect to the thermal correlation values.

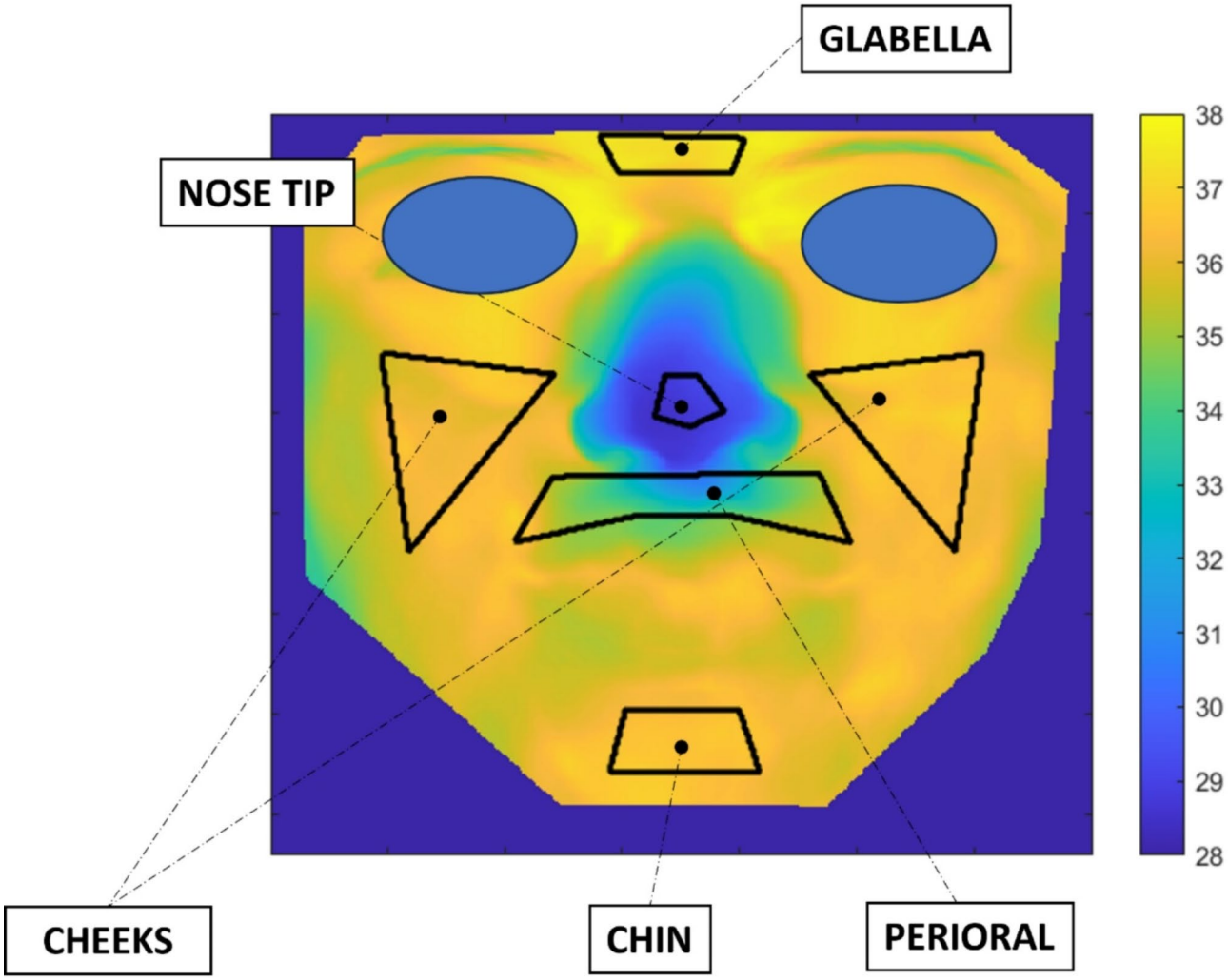

Fig. 11 . Representation of the ROIs locations used for the analysis on SCA maps. Particularly, the glabella, nose tip, cheeks, chin and perioral ROIs have been considered given their salient physiological meaning.

Data availability

The datasets used and/or analyzed during the current study are available from the corresponding author on reasonable request.

Received: 20 September 2024; Accepted: 25 February 2025
Published online: 02 March 2025

References

1. Cerritelli, F., Lacorte, E., Ruffini, N. & Vanacore, N. Osteopathy for primary headache patients: A systematic review. *J. Pain Res.* **10**, 601–611 (2017).
2. Cerritelli, F. et al. Osteopathic manipulation as a complementary treatment for the prevention of cardiac complications: 12-Months follow-up of intima media and blood pressure on a cohort affected by hypertension. *J. Bodyw. Mov. Ther.* **15**, 68–74 (2011).
3. Manzotti, A. et al. Neonatal assessment manual score: is there a role of a novel, structured Touch-Based evaluation in neonatal intensive care unit? *Front. Pediatr.* **8**, 1–10 (2020).
4. Bohlen, L., Shaw, R., Cerritelli, F. & Esteves, J. E. Osteopathy and mental health: an embodied, predictive, and interoceptive framework. *Front. Psychol.* **12**, 1–22 (2021).
5. Manzotti, A. et al. Effects of osteopathic treatment versus static touch on heart rate and oxygen saturation in premature babies: A randomized controlled trial. *Complement. Ther. Clin. Pract.* **39**, 101116 (2020).
6. Bohlen, L. et al. Effect of osteopathic techniques on human resting muscle tone in healthy subjects using myotonometry: a factorial randomized trial. *Sci. Rep.* **12**, 16953 (2022).
7. Manzotti, A. et al. Osteopathic manipulative treatment regulates autonomic markers in preterm infants: A randomized clinical trial. *Healthcare* **10**, 813 (2022).
8. Carnevali, L., Cerritelli, F., Guolo, F. & Sgoifo, A. Osteopathic manipulative treatment and cardiovascular autonomic parameters in rugby players: A randomized, Sham-Controlled trial. *J. Manip. Physiol. Ther.* **44**, 319–329 (2021).
9. Bagagiolo, D. et al. A randomized controlled trial of osteopathic manipulative therapy to reduce cranial asymmetries in young infants with nonsynostotic Plagiocephaly. *Am. J. Perinatol.* **39**, S52–S62 (2022).

10. Nguyen, C. et al. Effect of osteopathic manipulative treatment vs Sham treatment on activity limitations in patients with nonspecific subacute and chronic low back pain: A randomized clinical trial. *JAMA Intern. Med.* **181**, 620–630 (2021).
11. Ruffini, N. et al. Variations of high frequency parameter of heart rate variability following osteopathic manipulative treatment in healthy subjects compared to control group and Sham therapy: Randomized controlled trial. *Front. Neurosci.* **9**, 1–12 (2015).
12. D'Alessandro, G., Cerritelli, F. & Cortelli, P. Sensitization and interoception as key neurological concepts in osteopathy and other manual medicines. *Front. Neurosci.* **10**, 1–12 (2016).
13. Roura, S., Álvarez, G., Solà, I. & Cerritelli, F. Do manual therapies have a specific autonomic effect? An overview of systematic reviews. *PLoS ONE*. **16**, e0260642 (2021).
14. Cerritelli, F. et al. Osteopathy modulates brain–heart interaction in chronic pain patients: An ASL study. *Sci. Rep.* **11**, 4556 (2021).
15. Cerritelli, F. et al. Effect of manual approaches with osteopathic modality on brain correlates of interoception: An fMRI study. *Sci. Rep.* **10**, 3214 (2020).
16. Esteves, J. E., Cerritelli, F., Kim, J. & Friston, K. J. Osteopathic care as (En)active inference: A theoretical framework for developing an integrative hypothesis in osteopathy. *Front. Psychol.* **13**, 1–19 (2022).
17. Cerritelli, F. & Esteves, J. E. An enactive–ecological model to guide patient-centered osteopathic care. *Healthcare* **10**, 1092 (2022).
18. Licciardone, J. C., Kearns, C. M., Hodge, L. M. & Bergamini, M. V. W. Associations of cytokine concentrations with key osteopathic lesions and clinical outcomes in patients with nonspecific chronic low back pain: Results from the OSTEOPATHIC trial. *J. Osteopath. Med.* **112**, 596–605 (2012).
19. Degenhardt, B. F., Johnson, J. C., Fossum, C., Andicochea, C. T. & Stuart, M. K. Changes in cytokines, sensory tests, and Self-reported pain levels after manual treatment of low back pain. *Clin. Spine Surg.* **30**, E690 (2017).
20. Walkowski, S. et al. Osteopathic manipulative therapy induces early plasma cytokine release and mobilization of a population of blood dendritic cells. *PLoS ONE*. **9**, e90132 (2014).
21. Zein-Hammoud, M. & Standley, P. R. Modeled osteopathic manipulative treatments: A review of their in vitro effects on fibroblast tissue preparations. *J. Osteopath. Med.* **115**, 490–502 (2015).
22. McGlone, F., Cerritelli, F., Walker, S. & Esteves, J. The role of gentle touch in perinatal osteopathic manual therapy. *Neurosci. Biobehav. Rev.* **72**, 1–9 (2017).
23. Fornari, M., Carnevali, L. & Sgoifo, A. Single osteopathic manipulative therapy session dampens acute autonomic and neuroendocrine responses to mental stress in healthy male participants. *J. Osteopath. Med.* **117**, 559–567 (2017).
24. Cardone, D. & Merla, A. New frontiers for applications of thermal infrared imaging devices: Computational psychopshysiology in the neurosciences. *Sens. (Switzerland)* **17**, 1–21 (2017).
25. Ioannou, S., Gallese, V. & Merla, A. Thermal infrared imaging in psychophysiology: Potentialities and limits. *Psychophysiology* **51**, 951–963 (2014).
26. Krzywicki, A. T., Berntson, G. G. & O'Kane, B. L. A non-contact technique for measuring eccrine sweat gland activity using passive thermal imaging. *Int. J. Psychophysiol.* **94**, 25–34 (2014).
27. Cardone, D., Cerritelli, F., Chiacchiaretta, P., Perpetuini, D. & Merla, A. Facial functional networks during resting state revealed by thermal infrared imaging. *Phys. Eng. Sci. Med.* **16** https://doi.org/10.1007/s13246-023-01321-9 (2023).
28. Polidori, G., Kinne, M., Mereu, T., Beaumont, F. & Kinne, M. Medical infrared thermography in back pain osteopathic management. *Complement. Ther. Med.* **39**, 19–23 (2018).
29. Cerritelli, F., Cardone, D., Pirino, A., Merla, A. & Scoppa, F. Does osteopathic manipulative treatment induce autonomic changes in healthy participants? A thermal imaging study. *Front. NeuroSci.* **14**, 1–13 (2020).
30. D'Alessandro, G. et al. Overcoming placebo-related challenges in manual therapy trials: The 'whats and hows' and the 'touch equality assumption'proposals. *Int. J. Osteopath. Med.* **42**, 5–10 (2021).
31. Bingel, U. Placebo 2.0: The impact of expectations on analgesic treatment outcome. *Pain* **161**, S48 (2020).
32. Rossettini, G., Camerone, E. M., Carlino, E., Benedetti, F. & Testa, M. Context matters: The Psychoneurobiological determinants of placebo, Nocebo and context-related effects in physiotherapy. *Arch. Physiother*. **10**, 11 (2020).
33. Faraone, S. V. et al. Placebo and Nocebo responses in randomised, controlled trials of medications for ADHD: A systematic review and meta-analysis. *Mol. Psychiatry*. **27**, 212–219 (2022).
34. Skyt, I. et al. Neurotransmitter systems involved in placebo and Nocebo effects in healthy participants and patients with chronic pain: A systematic review. *Pain* **161**, 11 (2020).
35. Bardhan, S., Bhowmik, M. K., Nath, S. & Bhattacharjee, D. A review on inflammatory pain detection in human body through infrared image analysis. in *International Symposium on Advanced Computing and Communication (ISACC)* 251–257 (IEEE, 2015).
36. Ring, E. F. J. & Ammer, K. Infrared thermal imaging in medicine. *Physiol. Meas.* **33**, R33 (2012).
37. Sanchez, B. M. et al. Use of a portable thermal imaging unit as a rapid, quantitative method of evaluating inflammation and experimental arthritis. *J. Pharmacol. Toxicol. Methods*. **57**, 169–175 (2008).
38. Ju, X., Nebel, J. C. & Siebert, J. P. 3D thermography imaging standardization technique for inflammation diagnosis. *Infrared Compon. Their Appl.* **5640** (SPIE), 266–273 (2005).
39. Bhowmik, M. K., Bardhan, S., Das, K., Bhattacharjee, D. & Nath, S. Pain related inflammation analysis using infrared images. *Thermosense: Therm. Infrared Appl. XXXVIII*. **9861** (SPIE), 287–300 (2016).
40. Perpetuini, D., Formenti, D., Cardone, D., Filippini, C. & Merla, A. Regions of interest selection and thermal imaging data analysis in sports and exercise science: A narrative review. *Physiol. Meas.* **42**, 08TR01 (2021).
41. Gioia, F., Nardelli, M., Scilingo, E. P. & Greco, A. Autonomic regulation of facial temperature during stress: A Cross-Mapping analysis. *Sensors* **23**, 6403 (2023).
42. Cardone, D. et al. Classification of drivers' mental workload levels: Comparison of machine learning methods based on ECG and infrared thermal signals. *Sensors* **22**, 1–24 (2022).
43. Cerritelli, F., Chiacchiaretta, P., Gambi, F. & Ferretti, A. Effect of continuous touch on brain functional connectivity is modified by the operator's tactile attention. *Front. Hum. Neurosci.* **11**, 368 (2017).
44. D'Alessandro, G. et al. Five challenges for manual therapies trials with placebo controls: A proposal. *Int. J. Osteopath. Med.* **46**, 55–59 (2022).
45. Hohenschurz-Schmidt, D. et al. Recommendations for the development, implementation, and reporting of control interventions in efficacy and mechanistic trials of physical, psychological, and self-management therapies: The CoPPS Statement. *bmj* **381**, (2023).
46. Jacobs, G. A. Manual for the State-Trait Anxiety Inventory (Form Y) (Self-Evaluation Questionnaire). *Palo Alto* (1983).
47. Oldfield, R. C. The assessment and analysis of handedness: The Edinburgh inventory. *Neuropsychologia* **9**, 97–113 (1971).
48. Guest, S. et al. The development and validation of sensory and emotional scales of touch perception. *Atten. Percept. Psychophys.* **73**, 531–550 (2011).
49. Baltrušaitis, T., Robinson, P., Morency, L. P. & OpenFace An open source facial behavior analysis toolkit. in *IEEE Winter Conference on Applications of Computer Vision (WACV)* 1–10 (2016). https://doi.org/10.1109/WACV.2016.7477553
50. Cardone, D. et al. Automated warping procedure for facial thermal imaging based on features identification in the visible domain. *Infrared Phys. Technol.* **112**, 103595 (2021).
51. Cardone, D., Pinti, P., Di Donato, L. & Merla, A. Warping-based co-registration of thermal infrared images: Study of factors influencing its applicability. *Infrared Phys. Technol.* **83**, 142–155 (2017).
52. Cardone, D. et al. Driver stress state evaluation by means of thermal imaging: A supervised machine learning approach based on ECG signal. *Appl. Sci. (Switzerland)* **10**, 1–17 (2020).

53. Nicolini, Y. et al. Autonomic responses to emotional stimuli in children affected by facial palsy: The case of Moebius syndrome. *Neural Plast.* 1–13 (2019).
54. Boyko, N., Basystiuk, O. & Shakhovska, N. Performance Evaluation and comparison of software for face recognition, based on dlib and opencv library. in *IEEE Second International Conference on Data Stream Mining & Processing (DSMP)* 478–482 (2018). https://doi.org/10.1109/DSMP.2018.8478556
55. Eskimez, S. E., Maddox, R. K., Xu, C. & Duan, Z. Generating talking face landmarks from speech. in *Latent Variable Analysis and Signal Separation* (eds. Deville, Y., Gannot, S., Mason, R., Plumbley, M. D. & Ward, D.) 372–381 (Springer International Publishing, 2018).https://doi.org/10.1007/978-3-319-93764-9_35.
56. Morrone, G. et al. Face landmark-based speaker-independent audio-visual speech enhancement in multi-talker environments. in *ICASSP –2019 IEEE International Conference on Acoustics, Speech and Signal Processing (ICASSP)* 6900–6904 (2019). https://doi.org/10.1109/ICASSP.2019.8682061
57. Sharma, S., Shanmugasundaram, K. & Ramasamy, S. K. FAREC — CNN based efficient face recognition technique using Dlib. in *International Conference on Advanced Communication Control and Computing Technologies (ICACCCT)* 192–195 (2016). https://doi.org/10.1109/ICACCCT.2016.7831628
58. Perpetuini, D., Cardone, D., Filippini, C., Chiarelli, A. M. & Merla, A. Modelling impulse response function of functional infrared imaging for general linear model analysis of autonomic activity. *Sensors* **19**, 849 (2019).
59. Ogorevc, J., Geršak, G., Novak, D. & Drnovšek, J. Metrological evaluation of skin conductance measurements. *Measurement* **46**, 2993–3001 (2013).
60. Cousijn, J., Zanolie, K., Munsters, R. J. M., Kleibeuker, S. W. & Crone, E. A. The relation between resting state connectivity and creativity in adolescents before and after training. *PLoS ONE*. **9**, e105780 (2014).
61. Koyama, M. S., Ortiz-Mantilla, S., Roesler, C. P., Milham, M. P. & Benasich, A. A. A modulatory effect of brief passive exposure to non-linguistic sounds on intrinsic functional connectivity: Relevance to cognitive performance. *Cereb. Cortex*. **27**, 5817–5830 (2017).

Author contributions

F.C., A.M. and D.C. conceived the experiment, F.C, D.P. and D.C. conducted the experiment, F.C. and D.C. analysed the results, F.C. and D.C. wrote . wrote the manuscript in consultation with J.K., D.P. and A.M. All authors reviewed the manuscript.

Declarations

Competing interests

The authors declare no competing interests.

Additional information

Correspondence and requests for materials should be addressed to D.C.

Reprints and permissions information is available at www.nature.com/reprints.

Publisher's note Springer Nature remains neutral with regard to jurisdictional claims in published maps and institutional affiliations.